

Supporting Information for: S 2p and P 2p Core Level Spectroscopy of PPT Ambipolar Material and Its Building Block Moieties

E. Bernes,^a G. Fronzoni,^a, M. Stener,^a A. Guarnaccio,^b T. Zhang,^{c,d} C. Grazioli,^e

F. O. L. Johansson,^d M. Coreno,^b M. de Simone,^e C. Puglia,^{*,d} D. Toffoli,^{*,a}

^aDepartment of Chemical and Pharmaceutical Sciences, University of Trieste, 34127 Trieste, Italy

^bISM-CNR, Institute of Structure of Matter -Tito Scalo (PZ) and Trieste, Italy

^cSchool of Information and Electronics, MIIT Key Laboratory for Low-Dimensional Quantum Structure and Devices, Beijing Institute of Technology (BIT), Beijing 100081, China

^dDepartment of Physics and Astronomy, Uppsala University, Box 516, SE-751 20 Uppsala, Sweden

^eIOM-CNR, Laboratorio TASC, Sincrotrone Trieste, I-34149 Trieste, Basovizza, Italy

Table of Content

Table S1:	2
Table S2:	2
Fig. S1:	3
Fig. S2:	4
Fig. S3:	5
Fig. S4:	6
Fig. S5:	7
Fig. S6:	7
Fig. S7:	8
Optimized coordinates	9-11

Table S1. Comparison between experimental and theoretical S2p IPs for PPT and DBT. Theoretical IPs are obtained by using the B3LYP and LB94 xc potentials for PPT and DBT, respectively. Data for the latter are taken from ref.¹. See main text for the details about the basis sets used in the TDDFT calculations. All values are expressed in eV.

Edge	PPT		DBT	
	Theory ^a	Single fit	Theory ^b	Single fit
L_{II}	170.69	170.59	170.57	170.47
L_{III}	169.46	169.46	169.19	169.16
L_{III}	169.35	169.34	169.33	169.32

^aCalculated IPs shifted by +8.23 eV.

^bCalculated IPs shifted by -0.90 eV.

Table S2. Comparison between experimental and theoretical P2p IPs of TPPO and PPT. Theoretical IPs are obtained by using the B3LYP xc potential. See main text for the details about the basis sets used in the TDDFT calculations. All values are expressed in eV.

Edge	TPPO		PPT		
	Theory ^a	Single fit	Theory ^b		Single fit
			P1	P2	
L_{II}	138.21	138.15	138.22	138.14	138.01
L_{III}	137.28	137.28	137.33	137.32	137.22
L_{III}	137.27	137.27	137.22	137.20	137.10

^aCalculated IPs shifted by +8.17 eV.

^bCalculated IPs shifted by +7.91 eV.

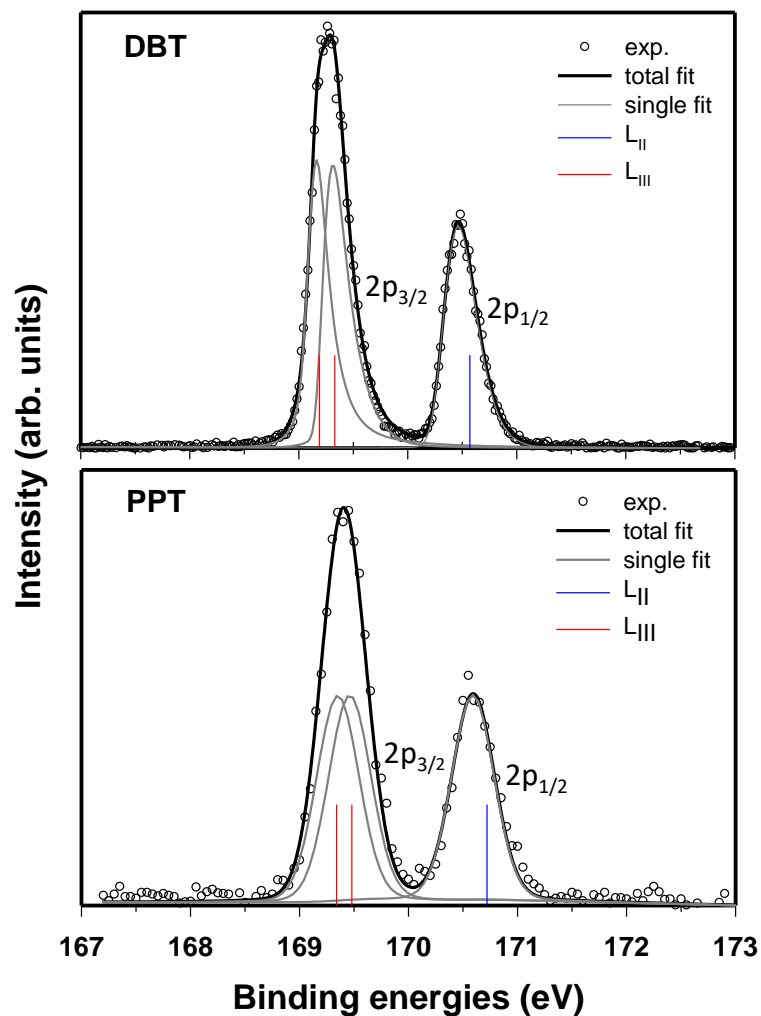


Figure S1. S_{2p} XP spectra of DBT (upper panel) and PPT (lower panel) calculated by employing the LB94 xc potential: experimental data (circles) are shown together with the results of the total fit (black line) obtained by the procedure described in the text. The vertical colored bars are the theoretical IPs and have been shifted by -0.90 eV and -1.23 eV for DBT and PPT, respectively. The light gray curves are the L_{II} (centered around the blue vertical bar) and L_{III} (centered around the red vertical bars) S_{2p} components obtained by the fitting procedure using a single and two asymmetric Voigt functions, respectively.

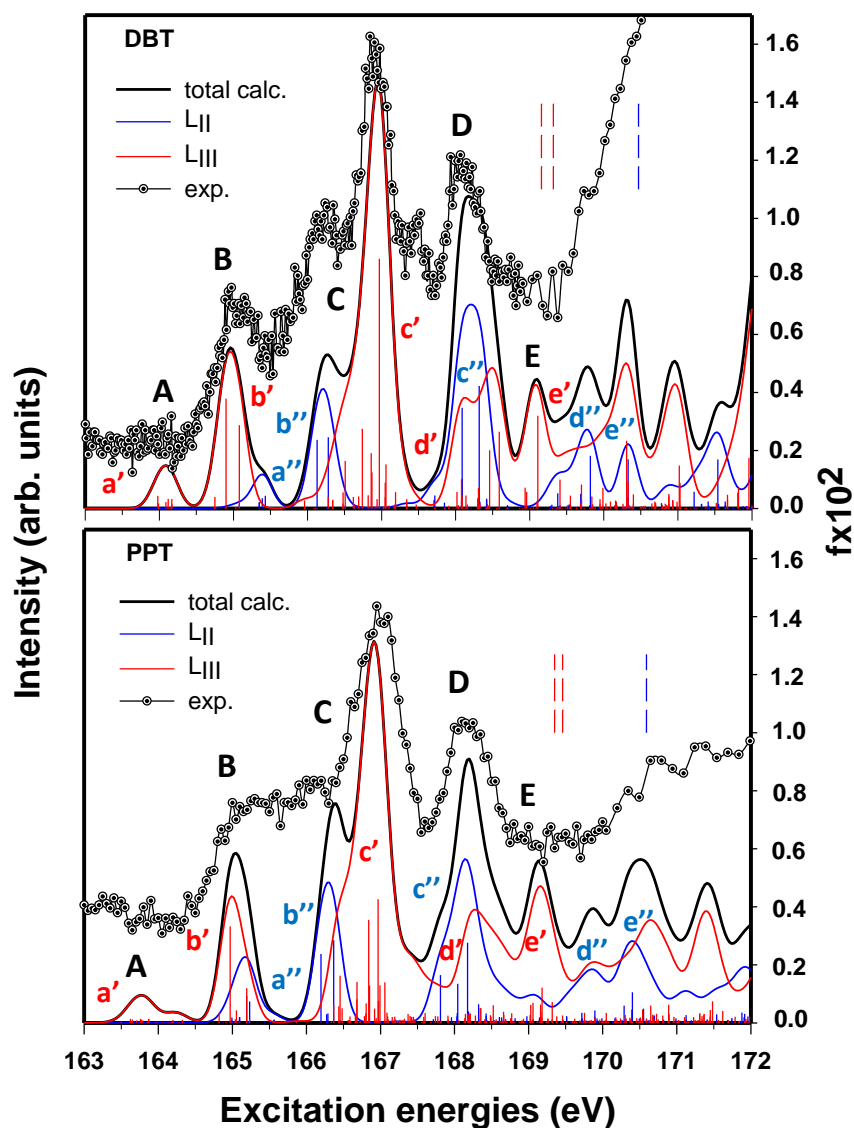


Figure S2. S $L_{II,III}$ -edge NEXAFS spectra of DBT (upper panel) and PPT (lower panel) calculated by employing the LB94 xc potential: experimental data (circles), calculated TDDFT results (black solid line). Also shown is the deconvolution of the calculated S2p spectrum into the two manifolds of excited states converging to the L_{III} (red solid line and vertical red bars) and L_{II} (blue solid line and vertical blue bars) edges. The energy scale of the calculated data has been shifted by +0.4 eV and +0.3 eV, respectively for DBT and PPT in order to match the first experimental peak. The experimental S2p ionization thresholds are also shown (blue and red vertical bars). The left vertical axis refers to the experimental intensities (plotted in arbitrary units), while the right vertical axis refers to computed oscillator strengths (multiplied by a factor of 100).

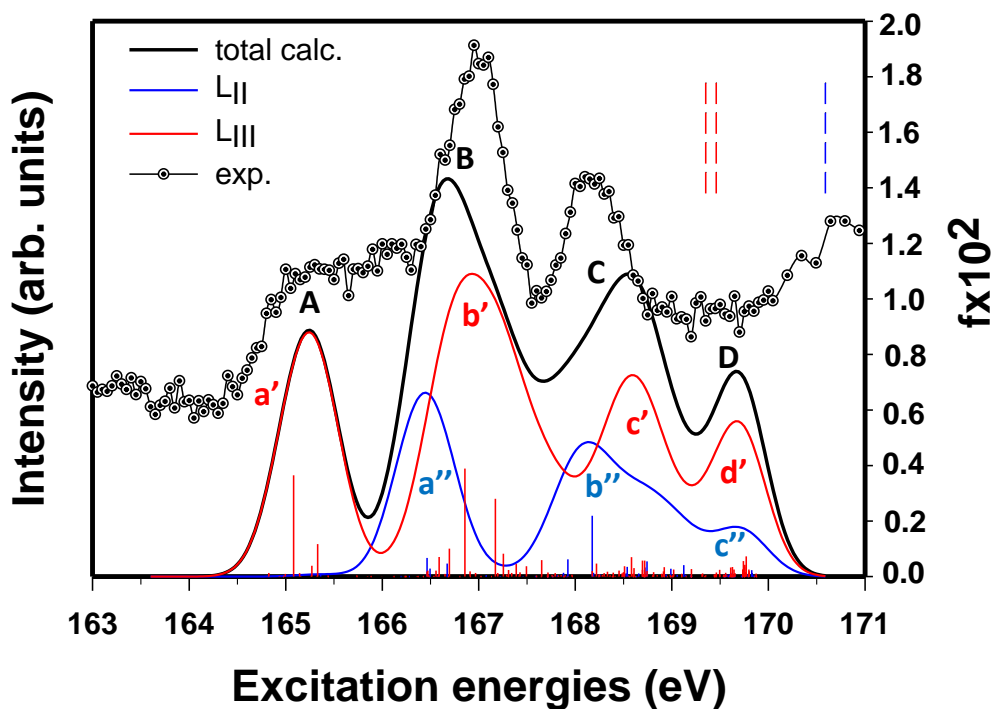


Figure S3. S $L_{II,III}$ -edge NEXAFS spectrum of PPT calculated by employing the hybrid B3LYP xc potential: experimental data (circles), calculated TDDFT results (black solid line). Also shown is the deconvolution of the calculated S2p spectrum into the two manifolds of excited states converging to the L_{III} (red solid line and vertical red bars) and L_{II} (blue solid line and vertical blue bars) edges. The energy scale of the calculated data has been shifted by +0.3 eV, in order to match the first experimental peak. The experimental S2p ionization thresholds are also shown (blue and red vertical bars). The left vertical axis refers to the experimental intensities (plotted in arbitrary units), while the right vertical axis refers to computed oscillator strengths (multiplied by a factor of 100).

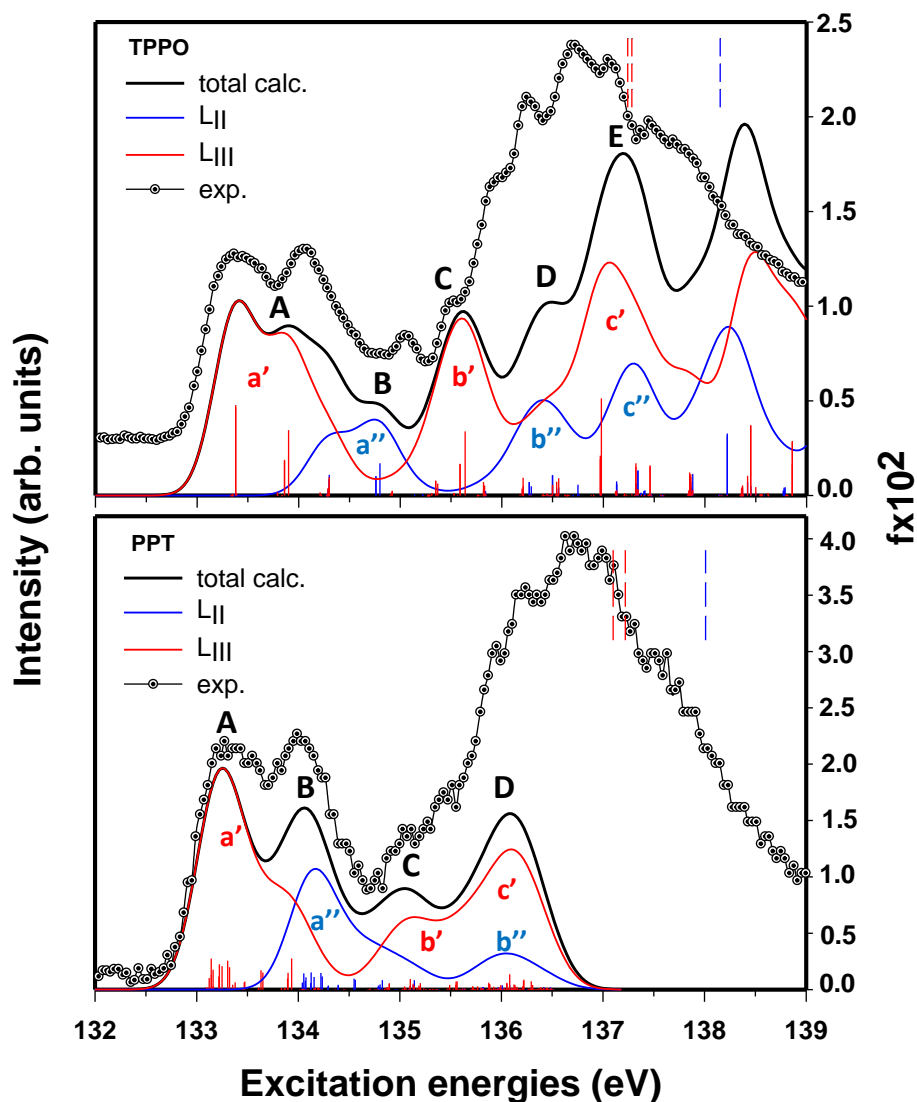


Figure S4. P $L_{II,III}$ -edge NEXAFS spectra of TPPO (upper panel) and PPT (lower panel) calculated by employing the hybrid B3LYP xc potential: experimental data (circles), calculated TDDFT results (black solid line). Also shown is the deconvolution of the calculated P2p spectrum into the two manifolds of excited states converging to the L_{III} (red solid line and vertical red bars) and L_{II} (blue solid line and vertical blue bars) edges. The energy scale of the calculated data has been shifted by +6.7 eV and +6.6 eV, respectively for TPPO and PPT in order to match the first experimental peak. The experimental P2p ionization thresholds are also shown (blue and red vertical bars). The left vertical axis refers to the experimental intensities (plotted in arbitrary units), while the right vertical axis refers to computed oscillator strengths (multiplied by a factor of 100).

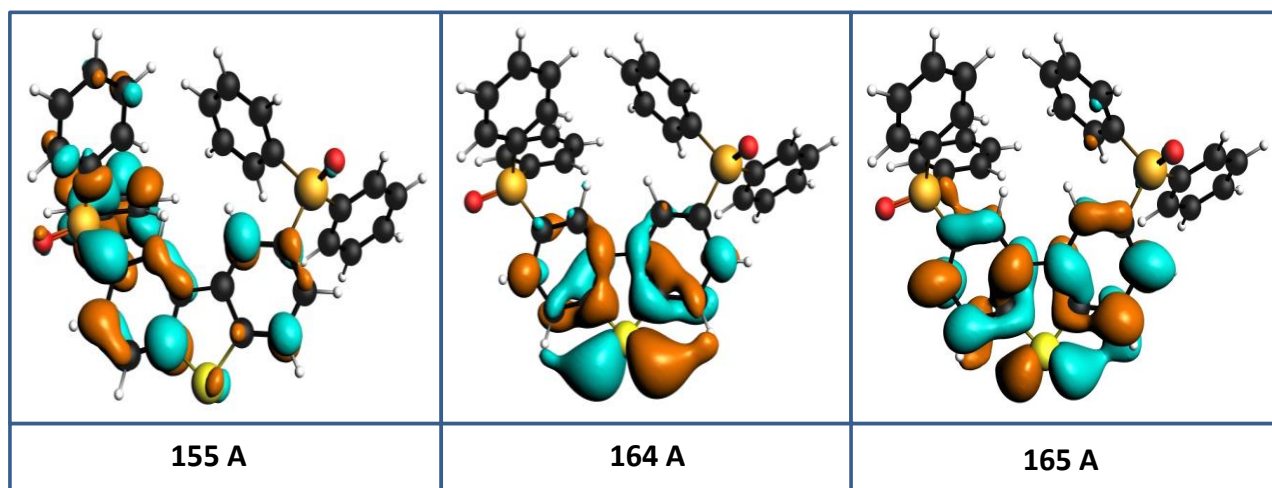


Figure S5. Plots of selected KS virtual molecular orbitals for PPT. For all atoms except S, an all-electron DZP basis set is used. A ET-QZ4P-2DIFFUSE basis is used for S. See main text for details about the basis set used in the TDDFT calculations.

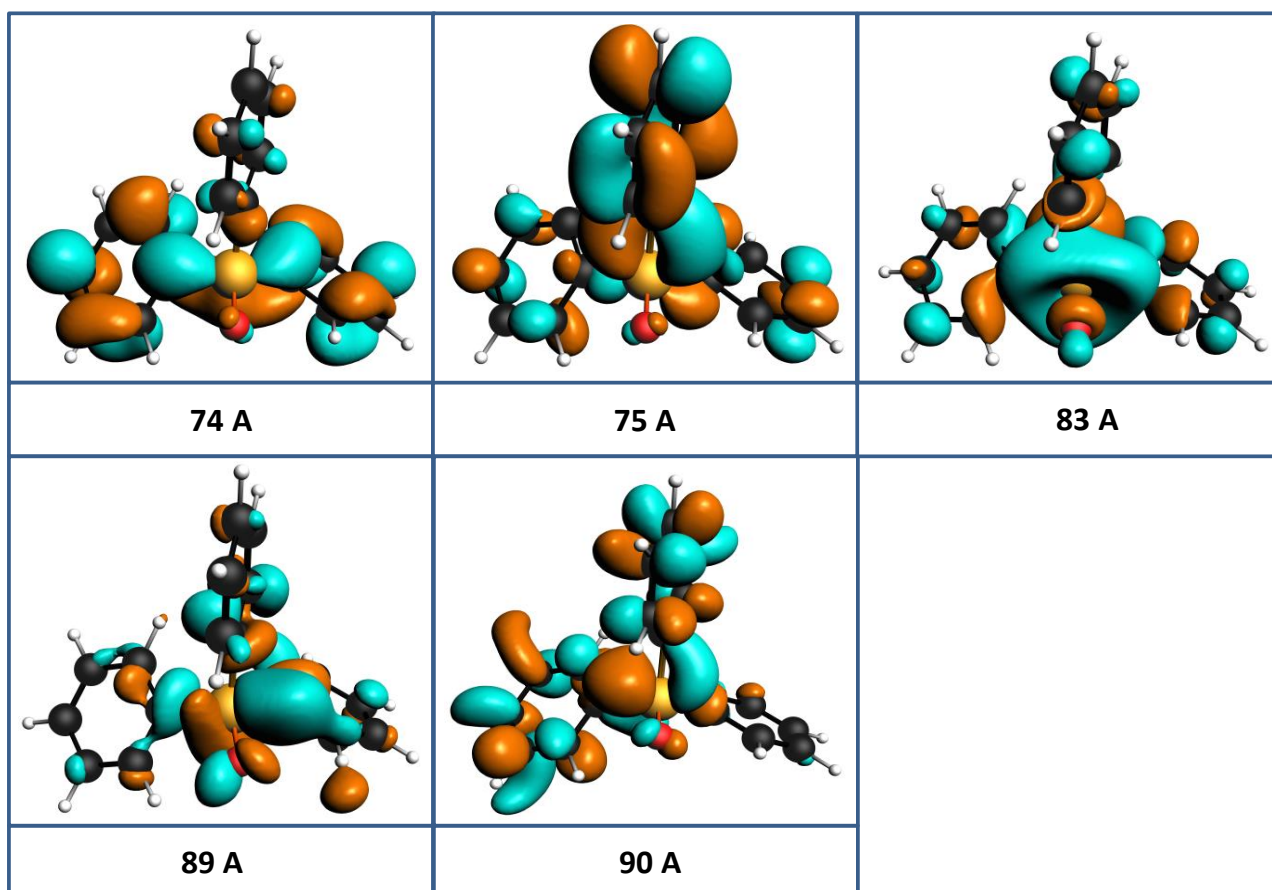


Figure S6. Plots of selected KS virtual molecular orbitals for TPPO. For all atoms except P, an all-electron DZP basis set is used. A ET-QZ4P-2DIFFUSE basis is used for P. See main text for details about the basis set used in the TDDFT calculations.

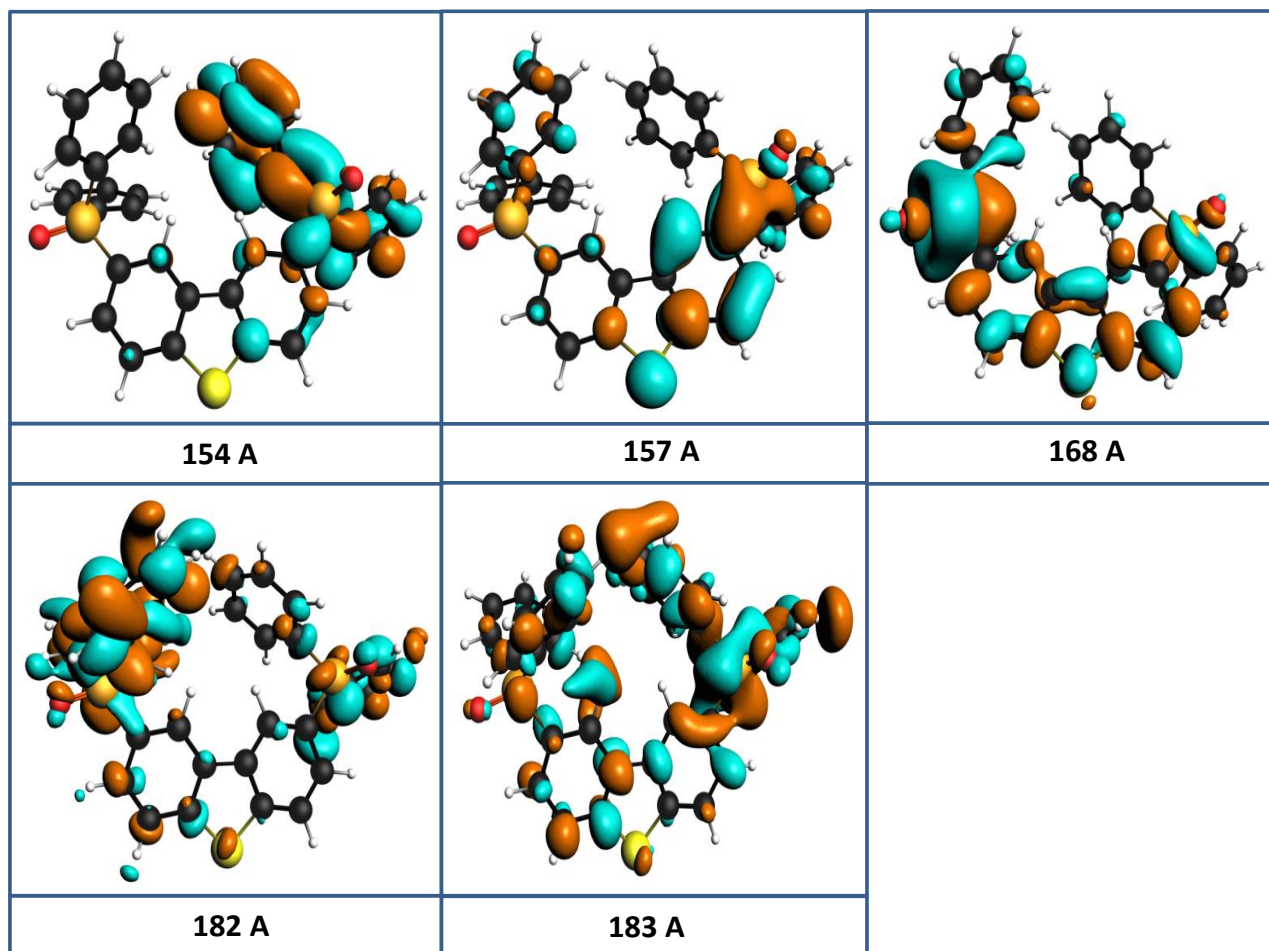


Figure S7. Plots of selected KS virtual molecular orbitals for PPT. For all atoms except P, an all-electron DZP basis set is used. A ET-QZ4P-2DIFFUSE basis is used for P. See main text for details about the basis set used in the TDDFT calculations.

Optimized Cartesian coordinates (in Å) of DBT, TPPO, and PPT.

DBT

S	0.165399	2.327192	0.000000
C	-0.727585	-0.129278	0.000000
C	0.703081	-0.230696	0.000000
C	-1.160065	1.206449	0.000000
C	1.319853	1.030856	0.000000
C	-1.679909	-1.143507	0.000000
C	1.500988	-1.370201	0.000000
C	-2.507545	1.533733	0.000000
C	2.700442	1.162621	0.000000
C	-3.022341	-0.823855	0.000000
C	2.875379	-1.245191	0.000000
C	-3.433981	0.508731	0.000000
C	3.471033	0.015890	0.000000
H	-1.358014	-2.189725	0.000000
H	1.032966	-2.359716	0.000000
H	-2.828436	2.578875	0.000000
H	3.167404	2.151159	0.000000
H	-3.771151	-1.620621	0.000000
H	3.503630	-2.140051	0.000000
H	-4.500771	0.748042	0.000000
H	4.561032	0.101408	0.000000

TPPO

P	-2.112017	0.995541	-1.057376
O	-2.118779	1.069084	-2.546294
C	-3.531391	1.810449	-0.321878
C	-0.657460	1.759385	-0.335448
C	-2.137326	-0.693132	-0.448509
C	-4.195507	2.728631	-1.126724
C	-5.301807	3.401281	-0.635924
C	-5.743352	3.159399	0.656643
C	-5.086596	2.235672	1.457421
C	-3.983609	1.555990	0.968390
C	0.435542	1.913688	-1.180239
C	-0.586349	2.188345	0.985459
C	-2.584066	-1.662567	-1.338917
C	-2.639311	-2.988499	-0.943441
C	-1.732482	-1.054216	0.832183
C	-2.251309	-3.346186	0.339564
C	-1.795832	-2.380429	1.225845
C	0.585062	2.751070	1.464214
C	1.602628	2.482600	-0.699186
C	1.679482	2.894704	0.623116
H	-5.830704	4.117214	-1.271641
H	-6.621757	3.686632	1.041159
H	-5.449590	2.029669	2.468347
H	-3.833948	2.880307	-2.149494
H	-3.492709	0.790434	1.580710
H	2.600585	3.349121	1.000669
H	0.639939	3.097205	2.500215
H	2.460482	2.612416	-1.365264

H	0.335628	1.595877	-2.223652
H	-1.327088	-0.296648	1.513125
H	-1.468693	-2.667126	2.229324
H	-2.289462	-4.395078	0.649136
H	-2.981941	-3.753367	-1.646274
H	-2.863524	-1.350418	-2.350907
H	-1.467815	2.116631	1.633414

PPT

C	-5.880226	-3.390747	3.920101
C	-0.379390	1.770507	3.305118
C	2.764076	4.108057	0.337233
C	3.894865	-1.135051	5.343652
C	-6.466789	-2.236315	3.422107
C	-4.585775	-3.731814	3.553459
C	-0.562401	0.434917	3.643024
C	-1.233405	2.380785	2.399361
C	2.068049	3.244082	1.170341
C	3.922121	3.680983	-0.295855
C	2.765457	-1.164650	4.537790
C	5.130648	-0.827826	4.794434
C	-5.757563	-1.415261	2.561759
C	-3.874297	-2.916213	2.689349
C	-1.582892	-0.293393	3.056810
C	-2.250192	1.650290	1.802155
C	2.526656	1.954403	1.371963
C	4.380549	2.388004	-0.104829
C	2.868245	-0.883690	3.186110
C	5.237436	-0.539238	3.443507
C	-2.990240	-2.746635	-0.597241
C	3.887604	-2.273208	-0.745764
C	-2.127038	-3.551671	-1.317416
C	3.112322	-3.200915	-1.417395
C	-1.170094	-1.329040	0.080082
C	1.922611	-1.095366	0.006404
C	-4.457672	-1.750963	2.201047
C	-2.415310	0.309416	2.118781
C	3.679623	1.520881	0.725260
C	4.105592	-0.560246	2.636933
C	-2.516186	-1.638590	0.120775
C	3.297091	-1.227726	-0.027262
C	-0.289410	-2.139580	-0.608779
C	1.132511	-2.039225	-0.628298
C	-0.766490	-3.257490	-1.302664
C	1.729119	-3.089376	-1.339906
O	-4.533993	0.299945	0.392647
O	5.791589	-0.218219	0.493656
P	-3.602590	-0.608582	1.116630
P	4.362925	-0.129251	0.907061
S	0.535151	-4.164732	-2.013752
H	-6.443030	-4.040109	4.597728
H	-7.491340	-1.976657	3.703565
H	-4.131229	-4.650730	3.934358
H	-6.196161	-0.505630	2.137915
H	-2.864902	-3.198724	2.367862
H	0.437855	2.339249	3.761234

H	0.107348	-0.038905	4.368042
H	-1.102883	3.437006	2.145455
H	-1.724282	-1.349768	3.312302
H	-2.927102	2.093658	1.063834
H	-4.057464	-2.988349	-0.572218
H	-2.508096	-4.418368	-1.862642
H	-0.780588	-0.464213	0.626232
H	2.404284	5.130524	0.186872
H	1.157492	3.577907	1.678242
H	4.477555	4.365732	-0.943047
H	1.991409	1.293235	2.065169
H	5.300792	2.027095	-0.576609
H	3.811846	-1.367909	6.409643
H	1.794336	-1.433250	4.966277
H	6.023825	-0.818481	5.425732
H	1.977360	-0.949208	2.550442
H	6.201769	-0.306419	2.978849
H	4.980264	-2.332447	-0.763615
H	3.581196	-4.011436	-1.980426
H	1.449630	-0.249858	0.519658

References

¹ Toffoli, D.; Guarnaccio, A.; Grazioli, C.; Zhang, T.; Johansson, F.; de Simone, M.; Coreno, M.; Santagata, A.; D'Auria, M.; Puglia, C. et al. Electronic Structure Characterization of a Thiophene Benzo-Annulated Series of Common Building Blocks for Donor and Acceptor Compounds Studied by Gas Phase Photoelectron and Photoabsorption Synchrotron Spectroscopies. *J. Phys. Chem. A* **2018**, *122*, 8745–8761